Resource

Cell Reports

An Epigenetic Memory of Pregnancy in the Mouse Mammary Gland

Graphical Abstract

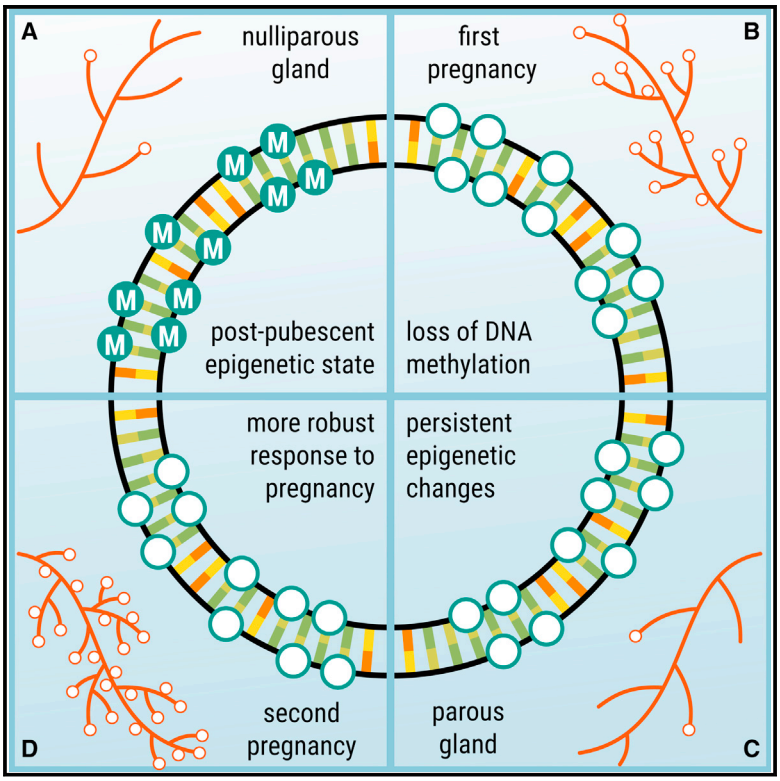

Authors

Camila O. dos Santos, Egor Dolzhenko, ..., Andrew D. Smith, Gregory J. Hannon

Correspondence

hannon@cshl.edu

In Brief

dos Santos et al. find that mammary glands from parous animals react more robustly to a subsequent pregnancy. This phenotype correlates with DNA methylation established during the first pregnancy cycle, the presence of which is associated with a rapid increase in gene expression of specific genes. Globally, these changes represent a memory of past pregnancies.

Highlights

- Glands from parous animals react more robustly to a subsequent pregnancy
- Pregnancy induces stable loss of DNA methylation in a Stat5a-biased fashion
- Loss of DNA methylation primes genes for rapid activation in a subsequent pregnancy

Accession Numbers

GSE67386

dos Santos et al., 2015, Cell Reports *11*, 1102–1109
May 19, 2015 ©2015 The Authors
http://dx.doi.org/10.1016/j.celrep.2015.04.015

OPEN ACCESS
CellPress

Cell Reports
Resource

An Epigenetic Memory of Pregnancy in the Mouse Mammary Gland

Camila O. dos Santos,[1,5] Egor Dolzhenko,[2,5] Emily Hodges,[1,3] Andrew D. Smith,[2] and Gregory J. Hannon[1,4,*]
[1]Howard Hughes Medical Institute, Watson School of Biological Sciences, Cold Spring Harbor Laboratory, 1 Bungtown Road, Cold Spring Harbor, NY 11724, USA
[2]Molecular and Computational Biology, University of Southern California, Los Angeles, CA 90089, USA
[3]Department of Biochemistry, Vanderbilt Genetics Institute, Vanderbilt University, Nashville, TN 37232-0146, USA
[4]Cancer Research UK Cambridge Institute, Li Ka Shing Centre, University of Cambridge, Robinson Way, Cambridge CB2 0RE, UK
[5]Co-first author
*Correspondence: hannon@cshl.edu
http://dx.doi.org/10.1016/j.celrep.2015.04.015

SUMMARY

Pregnancy is the major modulator of mammary gland activity. It induces a tremendous expansion of the mammary epithelium and the generation of alveolar structures for milk production. Anecdotal evidence from multiparous humans indicates that the mammary gland may react less strongly to the first pregnancy than it does to subsequent pregnancies. Here, we verify that the mouse mammary gland responds more robustly to a second pregnancy, indicating that the gland retains a long-term memory of pregnancy. A comparison of genome-wide profiles of DNA methylation in isolated mammary cell types reveals substantial and long-lasting alterations. Since these alterations are maintained in the absence of the signal that induced them, we term them epigenetic. The majority of alterations in DNA methylation affect sites occupied by the Stat5a transcription factor and mark specific genes that are upregulated during pregnancy. We postulate that the epigenetic memory of a first pregnancy primes the activation of gene expression networks that promote mammary gland function in subsequent reproductive cycles. More broadly, our data indicate that physiological experience can broadly alter epigenetic states, functionally modifying the capacity of the affected cells to respond to later stimulatory events.

INTRODUCTION

Pregnancy exerts pervasive physiological effects, in part by causing systemic exposure to pregnancy-associated hormones. Among the organs on which these hormonal effects have the greatest impact is the mammary gland. The mammary epithelium responds to pregnancy hormones by initiating a massive expansion. Through this program of proliferation and differentiation, thousands of ductal structures are formed, and these support milk production and transport during lactation.

Though most mammals rely on milk production to support their offspring, nursing can represent a source of great frustration in humans. Anecdotal evidence taken from the experience of mothers and lactation consultants indicates that, after a first pregnancy is completed, subsequent pregnancies are characterized by an improved nursing experience and increased milk supply (http://forums.llli.org/showthread.php?97789-Did-you-have-low-milk-supply-for-your-first-baby-and-not-your-2nd; http://www.essentialbaby.com.au/forums/index.php?/topic/807330-more-milk-with-second-baby/; http://www.whattoexpect.com/forums/breastfeeding/archives/is-it-true-u-produce-more-milk-with-yr-2nd-baby.html). A handful of scientific studies have also reported that humans have a significantly increased milk supply during a second pregnancy (De Amici et al., 2001; Ingram et al., 1999, 2001; Zuppa et al., 1988). In non-human mammals, multiple pregnancies have also been shown to increase milk supply and enhance lobulo-alveolar development (Byrnes and Bridges, 2005; Lang et al., 2012; Miller et al., 2006). Thus, evidence suggests that the mammary gland forms a long-term memory of pregnancy that alters its response to subsequent exposures to pregnancy hormones. Though the mechanisms underlying this memory are unclear, it has been suggested that parity might alter prolactin secretion as well as altering the sensitivity of responsive tissues to the hormone (Byrnes and Bridges, 2005; Lang et al., 2012).

The morphology of the post-involution gland of parous females is essentially indistinguishable from that of nulliparous animals. Thus, it is likely that pregnancy modifies the gland in a manner that does not derive from changes in its overall organization. We therefore hypothesized that pregnancy might alter the receptiveness of the gland to pregnancy-associated hormones and that this might be accomplished through long-lasting epigenetic modifications.

Here, we set out to determine the role of the mammary epigenome in how the gland reacts to the second pregnancy. We demonstrate that the parous mammary gland of a mouse, similar to humans and other mammals, responds more rapidly to the effects of a second pregnancy than the

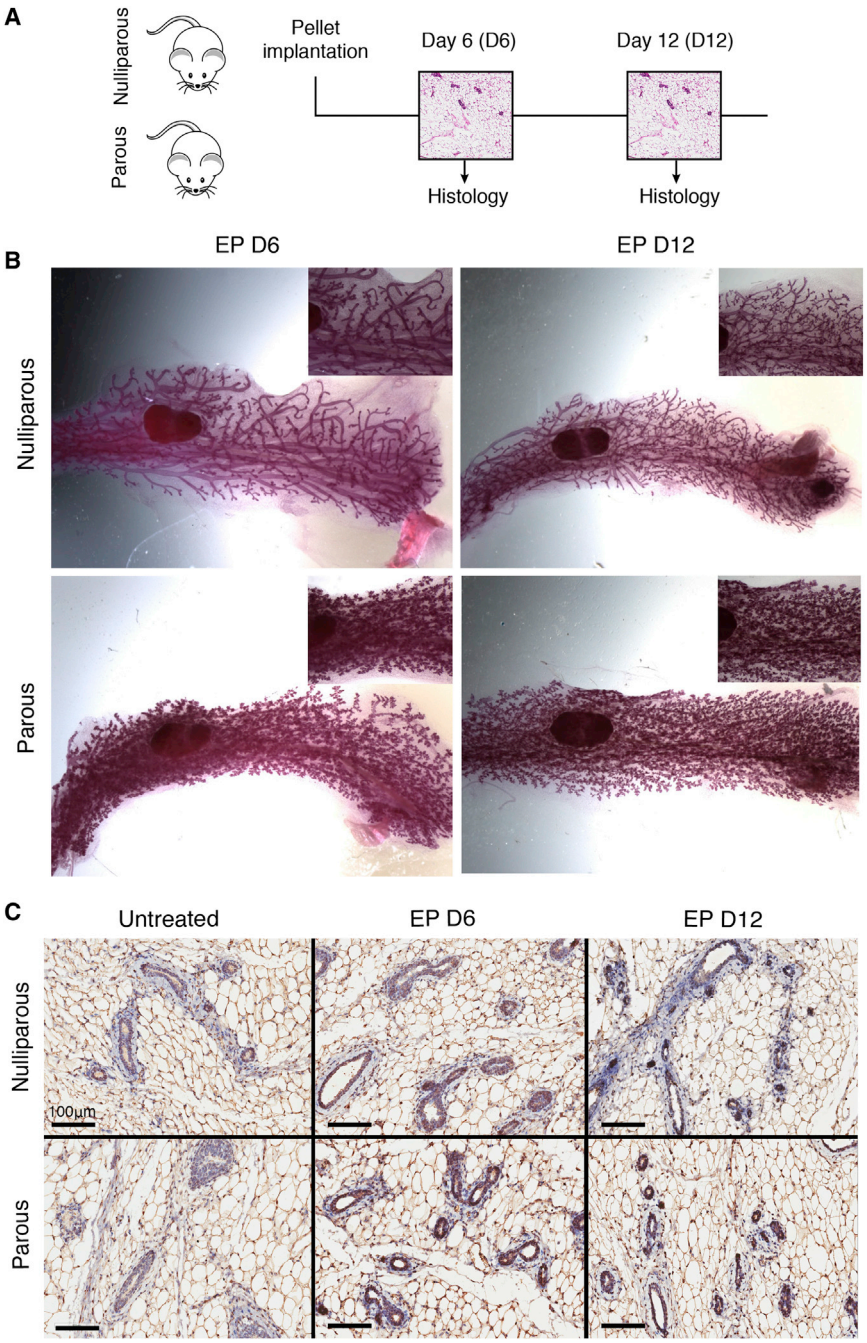

Figure 1. Increased Response of the Mammary Gland during a Second Pregnancy

(A) Experimental design. Nulliparous and parous mice were implanted with slow-release estrogen/progesterone pellets. Mammary glands from pellet-bearing mice were harvested at day 6 (D6) and day 12 (D12) after pellet implantation.

(B) Whole-mount images from pellet-bearing nulliparous and parous mice. Mammary glands were harvested, fixed, and cleared prior to Carmine staining.

(C) Glands from pellet-bearing nulliparous and parous mice were stained with an a-milk protein antibody.

nulliparous gland. This rapid response involves both the expansion of ductal structures and synthesis of milk proteins earlier in pregnancy.

Utilizing a comprehensive genomic approach, we profiled DNA methylation of all major mammary epithelial cells of post-pubescence (nulliparous) and post-pregnancy (parous) mice. Comparison of nulliparous and parous methylomes revealed substantial changes induced by parity. Many of these changes were localized near genes with a known role in milk production, cell proliferation, and apoptosis. Analysis of the parous epigenome provided a strong indication that Stat5a transcription factor plays an important role in protecting specific genomic regions from acquiring methylation after pregnancy. Through targeted experiments, we demonstrated that genes impacted by parity-associated epigenomic changes are poised for more rapid reactivation in a subsequent pregnancy. Collectively, our studies demonstrated the existence of an epigenetic memory of past pregnancies.

RESULTS AND DISCUSSION

Histological Evidence Shows that Mammary Glands from Parous Mice React Differently to a Subsequent Pregnancy

To assess the response of glands to repeated pregnancy, we exposed nulliparous mice (never pregnant) and parous mice (one pregnancy cycle, uniparous), to pregnancy-associated hormones. For these studies, parous animals had undergone a full cycle of pregnancy, birth, lactation, weaning, and involution. Nulliparous animals were age matched. We implanted these mice with slow-release estrogen/progesterone pellets. These release hormones at levels comparable to those measured during mouse pregnancy and successfully mimic the effects of pregnancy as evidenced by induction of ductal development and ultimately milk production (Silberstein et al., 1994). We harvested mammary glands on days 6 (D6) and 12 (D12) following implantation (Figure 1A).

Histological analysis confirmed that pseudo-pregnancy is sufficient to trigger ductal branching morphogenesis in mammary glands from both nulliparous and parous mice. However, glands of parous mice exhibited an earlier response to pregnancy hormones and showed elaboration of a greater number of ductal

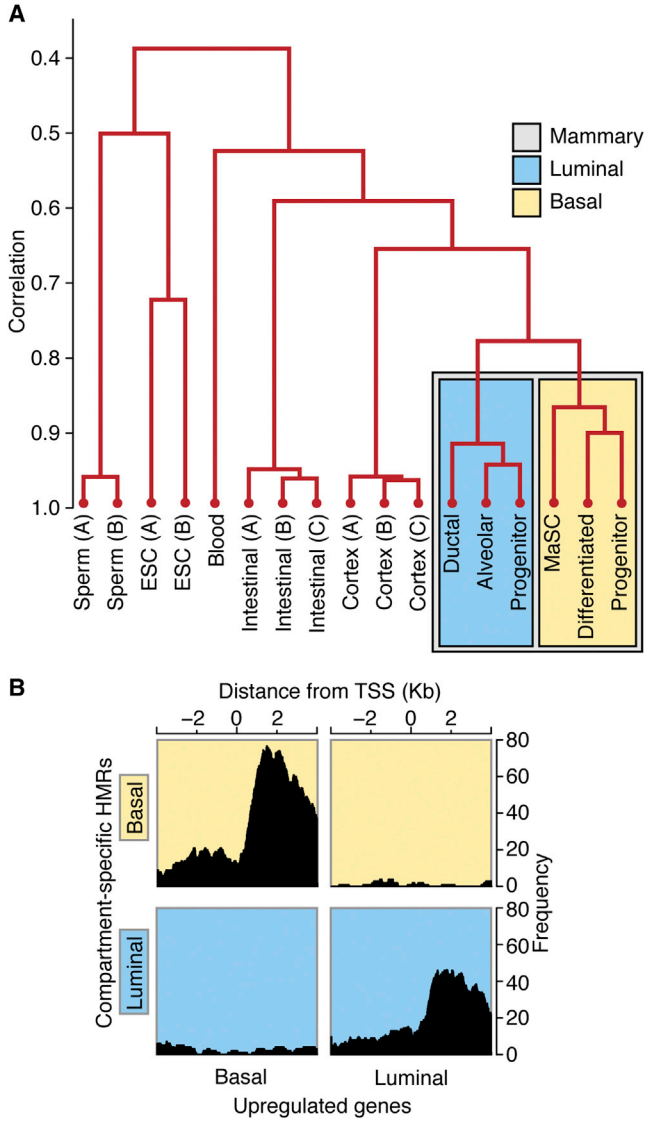

Figure 2. Genome-wide Methylation Profiles of Mammary Epithelial Cells

(A) Hierarchical clustering of genome-wide methylation profiles of mammary epithelial cells. Several other cell types are included for comparison.

(B) Relationship between compartment-specific HMRs and gene expression. The horizontal axes correspond to distances from transcription start sites (TSS) of genes with preferential expression in basal or luminal compartments. The height of each bar corresponds to the frequency of compartment-specific HMRs.

structures than did nulliparous mammary glands at each time point (Figures 1B and S1).

A prior pregnancy also influenced milk production. Glands from nulliparous and parous pellet-bearing mice were stained with an antibody that recognizes a variety of milk proteins (see Experimental Procedures). Glands from untreated animals, regardless of whether parous or nulliparous, did not express milk proteins (Figure 1C, untreated). Though milk production was initiated in both parous and nulliparous animals following hormone exposure, parous ducts functioned earlier. This was evidenced by the detection of milk protein signal in cells from parous mammary glands at the earliest time point post pellet implantation (Figure 1C, bottom). In contrast, mammary glands from nulliparous animals displayed a much weaker staining signal on day 6 (Figure 1C, top), suggesting that milk production by these animals is considerably delayed. At day 12, mammary glands from both parous and nulliparous female mice produced roughly equivalent amounts of milk proteins, at least to the sensitivity of the staining procedure (Figure 1C). Collectively, these results support the observation that mammary glands react differently to pregnancy hormones in mice that have experienced a prior pregnancy, just as they are thought to in other mammals.

Generation of the Mammary Reference Methylomes

Changes in the biology of the gland following pregnancy appear to be long lasting. We therefore hypothesized that differential responses might reflect epigenetic changes that prime gene expression programs in the parous gland to respond to future pregnancies. We focused on DNA methylation as the mark for which mechanisms of persistence are best understood. Moreover, changes in DNA methylation patterns are known to impact gene expression via a number of different mechanisms.

We generated single-nucleotide methylation profiles for all major mammary epithelial cell types from parous and nulliparous animals using whole-genome bisulfite sequencing. These included cells from the basal compartment: Cd1d MaSCs ($Lin^{-}CD24^{+}CD29^{h}CD61^{/l}Cd1d^{+}$), myoepithelial progenitors cells ($Lin^{-}CD24^{+}CD29^{h}CD61^{+}Cd1d^{-}$), myoepithelial differentiated cells ($Lin^{-}CD24^{+}CD29^{h}CD61^{-}Cd1d^{-}$); and cells from the luminal compartment: luminal progenitor cells ($Lin^{-}CD24^{h}CD29^{+}CD61^{+}CD133^{-}$), luminal ductal cells ($Lin^{-}CD24^{h}CD29^{+}CD61^{-}CD133^{+}$), and luminal alveolar cells ($Lin^{-}CD24^{h}CD29^{+}CD61^{-}CD133^{-}$).

We performed a hierarchical clustering of the methylation profiles of nulliparous mammary gland cells and a selected set of non-mammary cells consisting of embryonic stem cells (ESCs), brain cells, blood cells, sperm, and intestinal cells. This analysis revealed a shared epigenetic signature of mammary gland cells, distinct from those of the other cell types (Figure 2A). We observed a further separation of mammary methylation profiles into two distinct groups, corresponding to the luminal and the basal compartments, presumably reflecting the lineage split of the progenitors from which each of these cell types originate (Figure 2A). Cells in these compartments have previously been observed to segregate similarly based upon expression patterns (Charafe-Jauffret et al., 2006; dos Santos et al., 2013)

As with other somatic cell types analyzed to date, mammary methylomes exhibit discrete intervals of hypomethylation, punctuating the globally high background methylation. Using a previously described method (Hodges et al., 2011; Molaro et al., 2011; Schlesinger et al., 2013), we identified the set of hypomethylated regions (HMRs) in each methylome. HMRs correspond to regions with low methylation in the underlying population of cells and are a suitable basis for globally describing epigenetic alterations associated with mammary development. The number

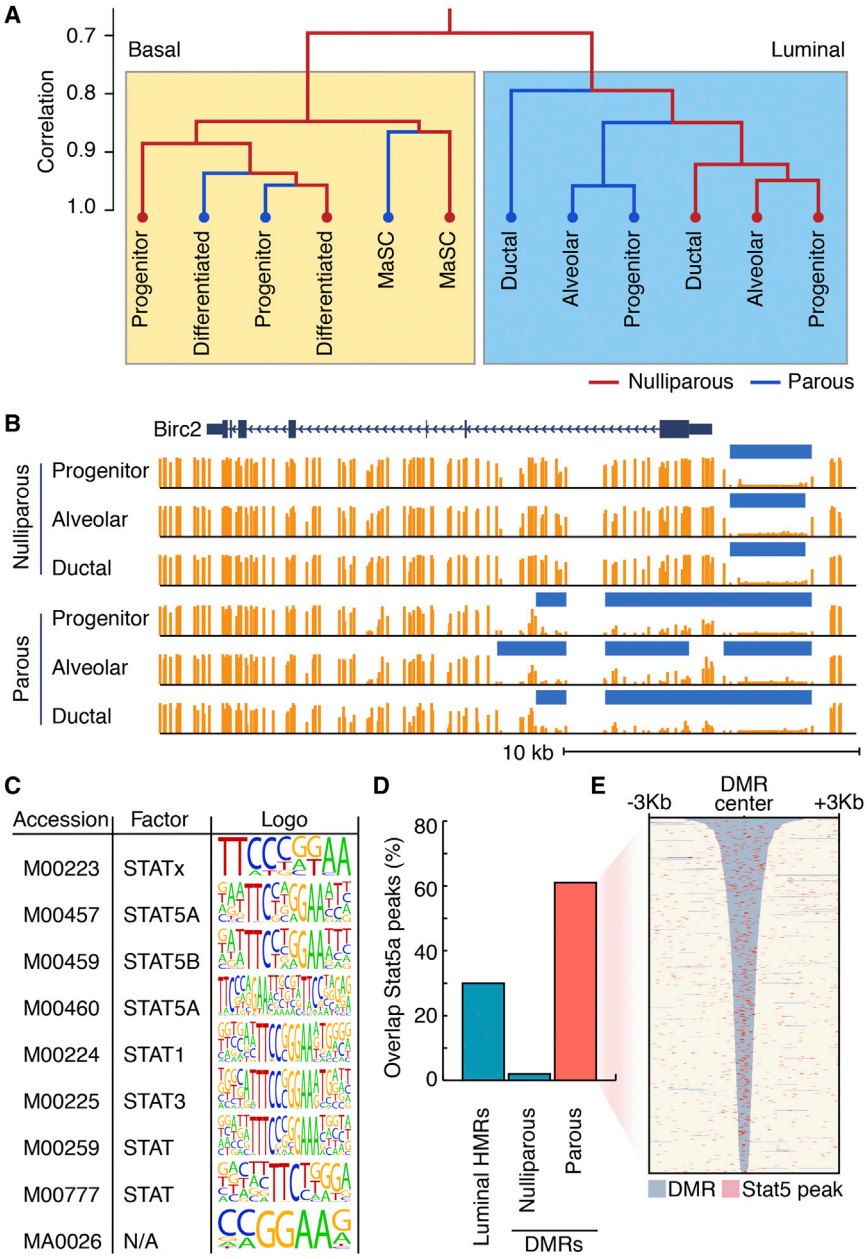

Figure 3. Pregnancy Leaves an Epigenetic Memory

(A) Hierarchical clustering of genome-wide methylation profiles from cells isolated from nulliparous and parous mice.

(B) Representative example of parity-induced DNA methylation changes at the Birc2 gene locus.

(C) Top ten transcription factor motifs significantly enriched at luminal parous DMRs.

(D) Bar graph showing the percentage of luminal HMRs, along with nulliparous- and parous-specific DMRs, that overlap with Stat5a peaks.

(E) Occupancy heatmap showing the distribution of Stat5a peaks at parous DMRs; the rows correspond to Stat5a occupancy across the parous luminal DMRs (±3 kb from DMR center); parous DMRs were sorted according to size (top, larger; bottom, shorter). The red lines correspond to Stat5a peaks and the gray lines represent the genomic regions spanned by DMRs.

of HMRs varied between 47k and 77k, with luminal cells tending to have larger HMRs (see the Supplemental Experimental Procedures).

Mammary epigenomes telegraph a strong compartmental identity. Analysis of the genomic locations of differentially methylated regions (DMRs) between the two mammary compartments indicated the association of compartment-specific HMRs with genes of known basal- and luminal-specific function (Figure S2). For example, cells from the basal compartment display lower levels of DNA methylation at the Krt5 gene, which encodes a basal-specific cytokeratin (Figure S2A, top), whereas the Krt8 gene, a cytokeratin preferentially expressed in luminal cells (Figure S2A, bottom), has significantly lower DNA methylation in luminal cells. Luminal and basal-specific HMRs in the promoter regions of differentially expressed genes correlated globally with their compartment-specific expression (Figure 2B).

Parity Reorganizes the Mammary Gland Epigenome

We next compared the methylation profiles of mammary gland cells from post-pregnancy animals to those of nulliparous animals. Our goal was to ask whether epigenetic alterations were induced by pregnancy and whether these persisted after the gland returns to its resting state following involution. Toward this end, we generated DNA methylation profiles for all mammary gland cell types harvested from multiparous females. These mice had undergone two complete gestational cycles, including pregnancy, lactation, and involution. To ensure that involution had been completed, glands were isolated 2 months after the end of lactation. We refer to these as parous samples from this point forward.

A genome-wide comparison of nulliparous and parous methylomes revealed that parity had a significant effect on the mammary epigenome (Figure 3A). Although all mammary methylomes retained their common compartmental identity, the individual cell types within each compartment from parous animals showed a significant divergence from their nulliparous counterparts. As an example, Figure S3A shows a region within the locus of the Dst gene—a gene with a pivotal role in cell adhesion integrity (Michael et al., 2014)—that had lost DNA methylation following pregnancy in every cell type (Figure S3A).

As a whole, the basal compartment was less affected by pregnancy. In fact, fewer than ten regions changed their methylation status simultaneously in more than one basal cell type. In contrast, the effect of parity on luminal methylomes was substantial. About 800 regions shared by all luminal cell types became hypomethylated in parous animals, whereas only 50 regions gained methylation (Figure S3B). The effect of pseudopregnancy (21 days of estrogen/progesterone pellet followed by 2 months involution) was sufficient to change the methylation status of luminal cells in a manner that is very similar to that of true pregnancy (Figure S3C). This is in agreement with the notion that luminal cells constitute the most abundant and most dynamic cell type in the mammary gland during pregnancy (Yamaji et al., 2009).

The methylation changes affecting luminal cells could reflect expression changes that underlie the expansion of ductal structures and alveoli during gestation, milk production during lactation, or remodeling during involution. Gene ontology analysis (McLean et al., 2010) revealed an association between regions that lost methylation with parity and genes with known roles in cell-cell adhesion, proliferation, and cell death (Figure S3D). An example can be seen in the Birc2 locus, a member of the IAP family of anti-apoptotic factors (Figure 3B). In this particular example, pregnancy triggered loss of DNA methylation over a 2-kb region around the Birc2 transcriptional start site (TSS). Other examples highlight gene families associated with parous DMRs, such as Itga, Stats, Tgf-β, and Wnt, that have already been demonstrated to be important during mammary gland development and pregnancy (Sternlicht et al., 2006) (Figures S4A–S4D). This suggests that the effects of pregnancy on the mammary gland epigenome may influence the expression of genes that regulate mammary gland homeostasis.

Other studies have profiled DNA methylation levels of nulliparous and parous mammary tissue, yet these used approaches that provide limited genomic coverage and bias for specific genomic regions (Choudhury et al., 2013; Huh et al., 2015). Our analysis of a published RRBS data set from the parous mouse mammary gland failed to detect the DNA methylation changes found by our high-resolution study (Figure S5). This discrepancy could be a consequence of the low genomic coverage of the RRBS data set at these specific regions. Nonetheless, this comparison supports the notion that genomic coverage and whole-genome analysis have a dramatic influence on the differentially methylated regions that can be identified.

We analyzed changes in methylation over known and predicted regulatory sequences to determine whether parous DMRs were associated with specific transcription factor binding sites. We found a strong enrichment for motifs recognized by the STAT family of transcription factors (Figure 3C). Stats are known to control a variety of biological processes in a diversity of cell types (Quintás-Cardama and Verstovsek, 2013). In the mammary gland, Stat5a/b are major modulators of cell proliferation during pregnancy, lactation, and involution. Deletion of both genes early in pregnancy allows normal alveolar development but hampers milk production (Cui et al., 2004). Furthermore, inhibition of Stat5a/b function late in pregnancy accelerates involution (Iavnilovitch et al., 2006). These developmental phenotypes may be a consequence of the deregulation of Stat5a/b downstream targets, where it acts either by transcriptional activation or repression. Recently, a direct correlation between gene regulation and Stat5a/b DNA occupancy in the mammary gland was suggested (Kang et al., 2014; Yamaji et al., 2013). These reports suggest that Stat5a/b act in two modes. In early pregnancy, low levels ensure the expansion of alveolar epithelium, whereas, early in the lactation phase, high levels activate differentiation and milk production.

To confirm the association between Stats and parity-associated methylation changes, we analyzed a Stat5a chromatin immunoprecipitation sequencing (ChIP-seq) data set obtained from a lactating mammary gland (Kang et al., 2014). About 63% of peaks overlapped HMRs present in both nulliparous and parous methylomes, and ~17% were present exclusively in parous methylomes. Only ~1% overlapped only with nulliparous-specific HMRs. The ~19% of peaks that did not overlap HMRs were still, on average, markedly less methylated in parous methylomes (Figure S6). These regions may represent methylation changes acquired by a subpopulation of cells, therefore becoming under-represented in our pool. It is also possible that some of the peaks reflect Stat5a occupancy in non-epithelial cells, which were not eliminated from the samples used for these ChIP-seq libraries (Kang et al., 2014). Together, our observations suggest that Stat5a activity during pregnancy has a functional relationship to the acquisition of a hypomethylated state at its binding sites, which is retained after pregnancy.

In addition to being associated with hypomethylated regions in parous methylomes, Stat5a peaks were present in 30% of HMRs shared by all luminal cells and 61% of parous DMRs (Figures 3D and 3E), reinforcing that idea that Stat5a is an important component controlling the epigenetic reorganization of luminal cells following pregnancy.

The Parous Epigenome Primes Genes for Re-activation in Subsequent Pregnancies

Mammary glands from parous mice react more quickly to pregnancy-associated signals (Figure 1). Additionally, many changes in the mammary epigenome induced by pregnancy occurred proximal to genes with known roles in mammary gland development, lactation, and involution. Yet, RNA sequencing (RNA-seq) indicated that the expression of these genes did not change in comparisons of glands from nulliparous versus parous mice (data not shown). We therefore hypothesized that durable changes in DNA methylation patterns might create a permissive environment for activation, essentially priming pregnancy-associated genes for rapid activation in response to subsequent pregnancies.

To address this hypothesis, we focused on 46 genes required for lactation and involution (Zhou et al., 2014). We first ascertained the mode of methylation change at each such gene as a function of parity in each mammary cell type (Figure 4A). Of the 46 genes analyzed, 33 genes were associated with parous-specific HMRs, whereas the Ccnd1 gene was the only one of these loci to acquire DNA methylation after pregnancy.

If the changes that we observe represent an epigenetic memory of pregnancy, then they should persist long after involution has returned the gland to a virgin-like state. We therefore purified the full spectrum of mammary epithelial cell types from mice that

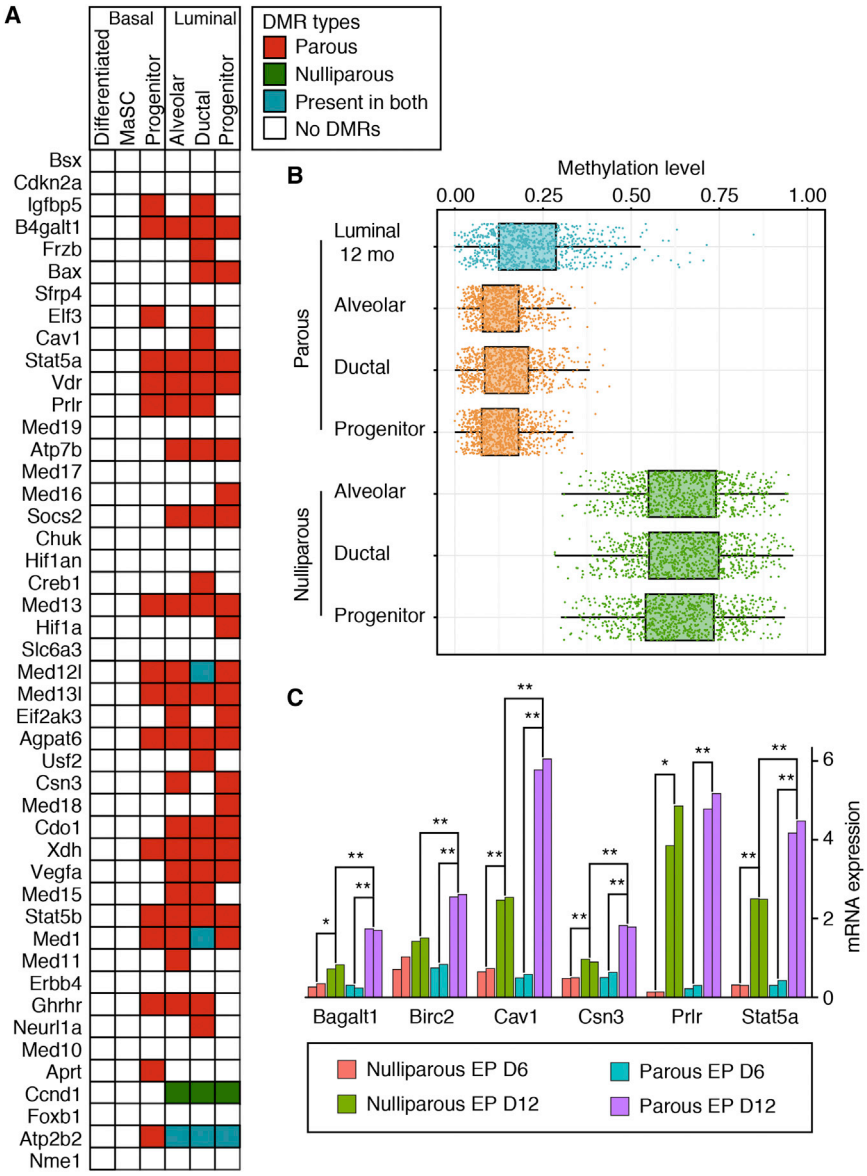

Figure 4. An Epigenetic Memory Primes Genes for Response in Subsequent Pregnancy

(A) The illustration shows the presence of nulliparous (green) and parous (red) DMRs within 4 kb of genes with role during lactation and involution. Genes with both nulliparous and parous DMRs are represented in blue (present in both). Genes with neither nulliparous nor parous DMRs are represented in white (no DMRs).

(B) Tukey boxplots of average DNA methylation levels of parous luminal DMRs in nulliparous luminal cells and luminal cells 2 and 12 months after pregnancy.

(C) Pregnancy hormones provoke enhanced activation of genes associated with parous DMRs. qPCR analysis is shown for nulliparous and parous mice at day 6 and 12 after implantation of hormone pellets. All changes were significant to at least $p < 0.05$.

had completed their last pregnancy 1 year prior to analysis. Focusing our investigation on the luminal compartment, we found that the vast majority of parous-specific HMRs, defined by their low methylation state 2 months after weaning, persisted throughout the majority of the mouse reproductive lifespan (Figure 4B). The persistence of these changes is remarkable, especially considering that the majority of luminal cells that are present during pregnancy are lost during involution and that there is continuous turnover within the luminal compartment during the mouse lifespan.

To ask whether the presence of persistent parous-specific HMRs had functional consequences for the gland, we asked whether genes associated with hypomethylated sites responded differently to pregnancy-associated hormones. We examined the expression patterns of several lactation genes that displayed parity-induced DNA methylation changes at the same time points shown in Figure 1. For comparison, we analyzed the expression of genes whose methylation state remained unchanged after pregnancy. As expected, pregnancy-associated changes in gene expression in the mammary gland occur in a time-dependent fashion, and the timing is consistent within groups of either nulliparous or parous animals (Figure 4C). The set of genes, which were not associated with pregnancy-specific HMRs, showed a similar time course of changes in expression throughout the experiment (Figure S7). However, genes with pregnancy-specific HMRs showed a greater degree of response in hormone-treated animals (Figure 4C). Thus, the stable epigenetic changes induced in the mammary epithelium by pregnancy prime genes for greater responses to hormone exposure, which may in turn result in the elaboration of a gland that functions more effectively during subsequent pregnancies.

Stable changes in patterns of DNA methylation have been proposed to reinforce cellular and tissue identity. This is consistent with studies of reference methylomes indicating that cell types within lineages cluster based upon state of their epigenome. Stable changes in DNA methylation that are heritable through mitotic and sometimes even meiotic divisions can underlie variations in phenotypic traits, and these have been termed epialleles. It has been proposed that the physiological experience of cells could leave stable epigenetic marks, which modify their behavior. In some ways, cellular differentiation driven by environmental signals would represent a clear example of such a phenomenon. Here, we have shown that the physiological experience of the mammary epithelium during pregnancy leaves a

long-term epigenetic memory that modifies both the behavior of the gland and the responses of the transcriptome to extracellular signals for essentially the reproductive life of the organism.

Changes in epigenetic state have been correlated with transcription factor binding, with occupancy by the factor predicting the presence of an HMR. However, in the absence of continued factor binding, hypomethylation tended to decay and the HMR was lost (Mohn et al., 2008). Our data suggest that, during pregnancy, engagement of Stat5a/b is similarly linked to the appearance of HMRs. Yet these HMRs persist, even when the gland returns to a resting, virgin-like state, a time when all measures of Stat5a/b activity suggest a return to pre-pregnancy baselines.

Considered as a whole, our data suggest that the physiological experience of pregnancy can leave an epigenetic memory that perdurantly modifies the mammary gland and perhaps other tissues, as well. It is well established that women who complete an early pregnancy gain a lifelong protection against breast cancer, a phenomenon that is conserved in other mammals. It is tempting to speculate that mechanisms similar to those that prime the activity of the gland for subsequent reproductive cycles might also underlie the modification of cancer risk. More broadly, our data clearly demonstrate that physiological experience can cause long-term alterations in epigenetic states that modify organ function, a paradigm that may come to be established as widespread as responses to other physiological stimuli are investigated.

EXPERIMENTAL PROCEDURES

Mice

Balb/C female mice (6–8 weeks old) were purchased from Charles River Laboratories. Parous mice were defined as those exposed to either one or two cycles of pregnancy-lactation-involution. All experiments were performed in agreement with approved by CSHL Institutional Animal Care and Use Committee.

Pellet Implantation

17β-estrogen (0.5 mg) and progesterone (10 mg) pellets (Innovative Research of America) were implanted in between the shoulder blades of age matching nulliparous and parous mice. Mammary glands of pellet-bearing mice were extracted at day 6 (D6) and day 12 (D12), post-pellet implantation.

Histology

Paraffin-embedded mammary gland sections were de-waxed and subjected to antigen retrieval in Trilogy buffer (Cell Marque), followed by blocking using 10% goat serum (Sigma-Aldrich). H&E staining was performed according to manufacturer's instructions (Sigma-Aldrich). Immunohistochemistry to detect milk proteins was performed using the Ace IHC Detection Kit (Epitomics) according to manufacture instructions. Antibody for immunohistochemistry was rabbit anti-milk-specific protein (Antibodies-online). Images were acquired using the Aperio ePathology (Leica Biosystems) slide scanner and ImageScope software (Leica Biosystems). For whole-mount images, glands were harvested, spread atop a glass slide, de-fated, and stained with Carmine Aluminum solution prior to image analysis.

Mammary Epithelial Cell Isolation

Mammary gland isolation and cell sorting were performed as previously described (dos Santos et al., 2013). In short, mammary glands were harvest from nulliparous (8–15 weeks old) parous (over 12 weeks old) and dissociated into single cells. After dissociation cells were stained with biotinylated anti-CD45, anti-Ter119 and anti-CD31 antibodies. Cells were then washed and further incubated with anti-biotin magnetic microbeads (Myltenyi Biotech). Labeled cells were loaded into a magnetic column attached to a magnetic field (Myltenyi Biotech), and lineage depleted cells were collected. Lineage depleted cells were stained with antibody mix for 30 min at 4°C with the following antibodies: anti-CD24 eFluor@ 450, PE-Cy7 conjugated anti-CD29, PE-conjugated anti-CD61, APC-conjugated anti-CD133, PerCP-CY5.5-conjugated anti-Cd1d (BioLegend), 7-AAD viability staining solution (BioLegend). All antibodies were purchased from eBioscience, unless otherwise specified. Fluorescence-activated cell sorting (FACS)-sorted cells were lysed with Lysis Buffer (10 mM Tris-HCl [pH 8], 2 mM EDTA, 1% SDS) followed by DNA purification.

Bisulfite Sequencing

Bisulfite sequencing libraries were generated as previously described (Hodges et al., 2011; Schlesinger et al., 2013). In short, purified genomic DNA was fragmented, adenylated, and ligated to Illumina-compatible paired-end adaptors. Bisulfite conversion was performed using the EZ DNA Methylation Gold kit (ZymoGenetics) according the manufacturer's instructions. Bisulfite converted, adaptor-ligated fragments were PCR enriched and further utilized on pair-ended Illumina sequencing. On average, we achieved an ~12-fold coverage of CpG sites (Supplemental Experimental Procedures) permitting us to accurately study features of individual methylomes and compare them to one another. Similar to other mammalian somatic cells, we observed globally high levels of methylation in these purified gland cells (Supplemental Experimental Procedures).

RNA Quantification

Mammary glands from pellet-bearing mice were harvest and digested with Collagenase/Hyaluronidase (STEMCELL Technologies). Digested tissue was further treated with 5 × Tripsin (Life Technologies) for 5 min. Nuclei were isolated using sucrose gradient (Yamaji et al., 2013) and lysed with 30 μl of Cell-To-Ct lysis buffer (Ambion). cDNA synthesis was performed according to manufacturer's instructions. Real-time PCR were performed on a 7900 Real-Time PCR System (Applied Biosystems). Gene-specific primers were designed using Primer Express (Applied Biosystems), and qPCRs were performed with SYBR Green. Gapdh mRNA was used as endogenous control.

Computational Analysis

Bisulfite treated read libraries were mapped with RMAP aligner (Smith et al., 2009) and subsequently processed using MethPipe methylation analysis pipeline (Song et al., 2013). Hypomethylated regions (HMRs) and differentially methylated regions (DMRs) were computed with MethPipe's hmr and dmr programs using default parameter values. Motif analysis was performed with CREAD (Smith et al., 2006) software. Stat5a ChIP-seq peaks were called as described in the original publication (Kang et al., 2014). A detailed description of computational methods can be found in the Supplemental Experimental Procedures.

ACCESSION NUMBERS

The NCBI GEO accession number for the genome-wide DNA methylation profiles of mammary epithelial cells reported in this paper is GSE67386.

SUPPLEMENTAL INFORMATION

Supplemental Information includes Supplemental Experimental Procedures, seven figures, and one table and can be found with this article online at http://dx.doi.org/10.1016/j.celrep.2015.04.015.

AUTHOR CONTRIBUTIONS

C.O.d.S., E.D, A.D.S., and G.J.H. designed research and wrote the paper; C.O.d.S. and E.H. performed experiments; C.O.d.S., E.D., and A.D.S. analyzed data; and E.D. and A.D.S. developed analysis methodology.

ACKNOWLEDGMENTS

We thank Antoine Molaro for helpful discussions. This work was performed with assistance from the CSHL Flow Cytometry Shared Resource and from the CSHL Histology Shared Resource, which are supported by Cancer Center Support Grant 5P30CA045508. This work was supported by the NIH Grand Opportunity award #1 RC2 CA148507 (G.J.H.), P01 award # 2P01CA013106 (G.J.H.), and NIH grant R01 H6005238 (A.D.S.). G.J.H. is an investigator of the Howard Hughes Medical Institute.

Received: February 17, 2015
Revised: March 20, 2015
Accepted: April 6, 2015
Published: May 7, 2015

REFERENCES

Byrnes, E.M., and Bridges, R.S. (2005). Lactation reduces prolactin levels in reproductively experienced female rats. Horm. Behav. *48*, 278–282.

Charafe-Jauffret, E., Ginestier, C., Monville, F., Finetti, P., Adélaïde, J., Cervera, N., Fekairi, S., Xerri, L., Jacquemier, J., Birnbaum, D., and Bertucci, F. (2006). Gene expression profiling of breast cell lines identifies potential new basal markers. Oncogene *25*, 2273–2284.

Choudhury, S., Almendro, V., Merino, V.F., Wu, Z., Maruyama, R., Su, Y., Martins, F.C., Fackler, M.J., Bessarabova, M., Kowalczyk, A., et al. (2013). Molecular profiling of human mammary gland links breast cancer risk to a p27(+) cell population with progenitor characteristics. Cell Stem Cell *13*, 117–130.

Cui, Y., Riedlinger, G., Miyoshi, K., Tang, W., Li, C., Deng, C.X., Robinson, G.W., and Hennighausen, L. (2004). Inactivation of Stat5 in mouse mammary epithelium during pregnancy reveals distinct functions in cell proliferation, survival, and differentiation. Mol. Cell. Biol. *24*, 8037–8047.

De Amici, D., Gasparoni, A., Guala, A., and Klersy, C. (2001). Does ethnicity predict lactation? A study of four ethnic communities. Eur. J. Epidemiol. *17*, 357–362.

dos Santos, C.O., Rebbeck, C., Rozhkova, E., Valentine, A., Samuels, A., Kadiri, L.R., Osten, P., Harris, E.Y., Uren, P.J., Smith, A.D., and Hannon, G.J. (2013). Molecular hierarchy of mammary differentiation yields refined markers of mammary stem cells. Proc. Natl. Acad. Sci. USA *110*, 7123–7130.

Hodges, E., Molaro, A., Dos Santos, C.O., Thekkat, P., Song, Q., Uren, P.J., Park, J., Butler, J., Rafii, S., McCombie, W.R., et al. (2011). Directional DNA methylation changes and complex intermediate states accompany lineage specificity in the adult hematopoietic compartment. Mol. Cell *44*, 17–28.

Huh, S.J., Clement, K., Jee, D., Merlini, A., Choudhury, S., Maruyama, R., Yoo, R., Chytil, A., Boyle, P., Ran, F.A., et al. (2015). Age- and pregnancy-associated DNA methylation changes in mammary epithelial cells. Stem Cell Reports *4*, 297–311.

Iavnilovitch, E., Eilon, T., Groner, B., and Barash, I. (2006). Expression of a carboxy terminally truncated Stat5 with no transactivation domain in the mammary glands of transgenic mice inhibits cell proliferation during pregnancy, delays onset of milk secretion, and induces apoptosis upon involution. Mol. Reprod. Dev. *73*, 841–849.

Ingram, J.C., Woolridge, M.W., Greenwood, R.J., and McGrath, L. (1999). Maternal predictors of early breast milk output. Acta Paediatr. *88*, 493–499.

Ingram, J., Woolridge, M., and Greenwood, R. (2001). Breastfeeding: it is worth trying with the second baby. Lancet *358*, 986–987.

Kang, K., Yamaji, D., Yoo, K.H., Robinson, G.W., and Hennighausen, L. (2014). Mammary-specific gene activation is defined by progressive recruitment of STAT5 during pregnancy and the establishment of H3K4me3 marks. Mol. Cell. Biol. *34*, 464–473.

Lang, S.L., Iverson, S.J., and Bowen, W.D. (2012). Primiparous and multiparous females differ in mammary gland alveolar development: implications for milk production. J. Exp. Biol. *215*, 2904–2911.

McLean, C.Y., Bristor, D., Hiller, M., Clarke, S.L., Schaar, B.T., Lowe, C.B., Wenger, A.M., and Bejerano, G. (2010). GREAT improves functional interpretation of cis-regulatory regions. Nat. Biotechnol. *28*, 495–501.

Michael, M., Begum, R., Fong, K., Pourreyron, C., South, A.P., McGrath, J.A., and Parsons, M. (2014). BPAG1-e restricts keratinocyte migration through control of adhesion stability. J. Invest. Dermatol. *134*, 773–782.

Miller, N., Delbecchi, L., Petitclerc, D., Wagner, G.F., Talbot, B.G., and Lacasse, P. (2006). Effect of stage of lactation and parity on mammary gland cell renewal. J. Dairy Sci. *89*, 4669–4677.

Mohn, F., Weber, M., Rebhan, M., Roloff, T.C., Richter, J., Stadler, M.B., Bibel, M., and Schübeler, D. (2008). Lineage-specific polycomb targets and de novo DNA methylation define restriction and potential of neuronal progenitors. Mol. Cell *30*, 755–766.

Molaro, A., Hodges, E., Fang, F., Song, Q., McCombie, W.R., Hannon, G.J., and Smith, A.D. (2011). Sperm methylation profiles reveal features of epigenetic inheritance and evolution in primates. Cell *146*, 1029–1041.

Quintás-Cardama, A., and Verstovsek, S. (2013). Molecular pathways: Jak/STAT pathway: mutations, inhibitors, and resistance. Clin. Cancer Res. *19*, 1933–1940.

Schlesinger, F., Smith, A.D., Gingeras, T.R., Hannon, G.J., and Hodges, E. (2013). De novo DNA demethylation and noncoding transcription define active intergenic regulatory elements. Genome Res. *23*, 1601–1614.

Silberstein, G.B., Van Horn, K., Shyamala, G., and Daniel, C.W. (1994). Essential role of endogenous estrogen in directly stimulating mammary growth demonstrated by implants containing pure antiestrogens. Endocrinology *134*, 84–90.

Smith, A.D., Sumazin, P., Xuan, Z., and Zhang, M.Q. (2006). DNA motifs in human and mouse proximal promoters predict tissue-specific expression. Proc. Natl. Acad. Sci. USA *103*, 6275–6280.

Smith, A.D., Chung, W.Y., Hodges, E., Kendall, J., Hannon, G., Hicks, J., Xuan, Z., and Zhang, M.Q. (2009). Updates to the RMAP short-read mapping software. Bioinformatics *25*, 2841–2842.

Song, Q., Decato, B., Hong, E.E., Zhou, M., Fang, F., Qu, J., Garvin, T., Kessler, M., Zhou, J., and Smith, A.D. (2013). A reference methylome database and analysis pipeline to facilitate integrative and comparative epigenomics. PLoS ONE *8*, e81148.

Sternlicht, M.D., Kouros-Mehr, H., Lu, P., and Werb, Z. (2006). Hormonal and local control of mammary branching morphogenesis. Differentiation *74*, 365–381.

Yamaji, D., Na, R., Feuermann, Y., Pechhold, S., Chen, W., Robinson, G.W., and Hennighausen, L. (2009). Development of mammary luminal progenitor cells is controlled by the transcription factor STAT5A. Genes Dev. *23*, 2382–2387.

Yamaji, D., Kang, K., Robinson, G.W., and Hennighausen, L. (2013). Sequential activation of genetic programs in mouse mammary epithelium during pregnancy depends on STAT5A/B concentration. Nucleic Acids Res. *41*, 1622–1636.

Zhou, Y., Gong, W., Xiao, J., Wu, J., Pan, L., Li, X., Wang, X., Wang, W., Hu, S., and Yu, J. (2014). Transcriptomic analysis reveals key regulators of mammogenesis and the pregnancy-lactation cycle. Science China. Life Sci. *57*, 340–355.

Zuppa, A.A., Tornesello, A., Papacci, P., Tortorolo, G., Segni, G., Lafuenti, G., Moneta, E., Diodato, A., Sorcini, M., and Carta, S. (1988). Relationship between maternal parity, basal prolactin levels and neonatal breast milk intake. Biol. Neonate *53*, 144–147.

Cell Reports

Supplemental Information

An Epigenetic Memory of Pregnancy in the Mouse Mammary Gland

Camila O. dos Santos, Egor Dolzhenko, Emily Hodges, Andrew D. Smith, and Gregory J. Hannon

Supplemental Methods

Initial processing of WGBS libraries

Bisulfite treated read libraries were processed using MethPipe methylation analysis pipeline as described here http://smithlabresearch.org/manuals/methpipe-manual.pdf. Briefly, 10 bp or longer sequences at either end of a read matching the sequencing adapter were trimmed. Then the trimmed reads were mapped with RMAP (Smith et al., 2009) aligner using *T to C* and the complimentary *A to G* wildcards to account for nucleotide substitutions during bisulfite treatment. The mm9 reference genome used for mapping was downloaded from UCSC Genome Browser and processed to exclude chromosomes annotated as "random" or "unassembled". To prevent PCR over-amplification bias, only one read from any set of identical reads mapping to the same location was kept.

We have processed 12 samples from basal (stem cells, progenitors, and differentiated cell types) and luminal (progenitor, alveolar, and ductal cell types) compartments (dos Santos et al., 2013) of nulliparous and parous mice. The estimated bisulfite conversion rate for all samples was above 98% (see Table 1 for other statistics). Hypomethylated regions (HMRs) were computed for each sample with MethPipe's hmr program used at default settings.

Pregnancy status	Cell type	average DNA methylation	% CpGs coverage	average coverage (X)	Hypomethylated regions (HMRs)
Nulliparous (virgin)	Stem cells (MaSC)	0.66	92	9.73	47,165
	Myo. progenitors	0.66	93	15.65	49,359
	Myo. differentiated	0.67	93	14.14	76,896
	Luminal progenitors	0.7	92	18.61	72,719
	Luminal alveolar	0.72	92	11.21	60,558
	Luminal ductal	0.72	92	14.15	61,592
Parous (2 months post pregnancy)	Stem cells (MaSC)	0.71	88	4.67	42,711
	Myo. progenitors	0.64	93	17.76	80,664
	Myo. differentiated	0.69	91	8.87	72,245
	Luminal progenitors	0.7	92	12.25	73,189
	Luminal alveolar	0.69	92	10.94	68,729
	Luminal ductal	0.69	92	10.48	65,964

Table 1: Average methylation level, percent of CpG sites covered by at least one read, average CpG site coverage, and the number of HMRs for the mammary gland samples sequenced and analyzed in the context of this project.

STAT5 peak calling

STAT5 ChIP-seq analysis was performed as described in the paper introducing the dataset (Kang et al., 2014). The reads were mapped with Bowtie aligner (Langmead et al., 2009) and peaks were called with HOMER (Heinz et al., 2010) at 0.001 FDR cutoff.

Motif enrichment

Motif enrichment analysis was performed with CREAD (Smith et al., 2006) software using a database of 775 known motifs from JASPAR (Sandelin et al., 2004) and TRANSFAC (Matys et al., 2006) databases. The analysis was performed using two sets of background sequences: (a) sequences upstream- and downstream- adjacent to the target sequences and (b) sequences obtained by randomly shuffling the order of nucleotides in the target sequences. For all sets of sequences analyzed here, both computations yielded very similar results (which was never the case when, as a control, we ran the same analysis on random sets of intervals from similar genomic locations). The specific order of the motifs presented in Figure 3 is based on the analysis using adjacent sequence background, however the same motifs appeared in top 10 when shuffled background was used.

Differential expression

We compared expression in the basal (5 RNA-seq samples) and luminal (5 RNA-seq samples) compartments of nulliparous mammary gland using edgeR software (Robinson et al., 2010). To do this, we filtered out all genes with read count per million (cpm) below 1 in more than 5 samples and used 0.01 significance cutoff to call differentially expressed genes (decideDGE function).

Genome annotations
Annotations of all genomic intervals were performed as follows: All intervals lying within 1Kb of REFSEQ TSS were classified as promoter intervals, and then the remaining intervals lying within 10Kb of gene bodies were classified as genic. All other intervals were classified as intergenic.

Dendrograms
To compute dendrograms, we separated the genome into 1Kb intervals and discarded the intervals with no coverage in at least one of the target WGBS samples. Then we associated a vector to each sample obtained by computing its average methylation levels in each interval. Using Pearson's correlation as a similarity measure (which was always positive), we used R's hclust function to perform a hierarchical clustering.

DMRs between a pair of methylomes
DMRs were computed using dmr program in MethPipe, which was ran with default parameters. For all analyses we kept DMRs spanning at least 10 CpG with at least 5 differentially methylated CpGs.

8) Luminal nulliparous/parous DMRs
To compute regions whose methylation was affected by pregnancy in all luminal methylomes, we first computed the DMRs for each luminal cell type (progenitor, alveolar, and ductal) separately, and then found their common intersection.

References

dos Santos, C.O., Rebbeck, C., Rozhkova, E., Valentine, A., Samuels, A., Kadiri, L.R., Osten, P., Harris, E.Y., Uren, P.J., Smith, A.D., et al. (2013). Molecular hierarchy of mammary differentiation yields refined markers of mammary stem cells. Proceedings of the National Academy of Sciences of the United States of America 110, 7123-7130.

Heinz, S., Benner, C., Spann, N., Bertolino, E., Lin, Y.C., Laslo, P., Cheng, J.X., Murre, C., Singh, H., and Glass, C.K. (2010). Simple combinations of lineage-determining transcription factors prime cis-regulatory elements required for macrophage and B cell identities. Molecular cell 38, 576-589.

Kang, K., Yamaji, D., Yoo, K.H., Robinson, G.W., and Hennighausen, L. (2014). Mammary-specific gene activation is defined by progressive recruitment of STAT5 during pregnancy and the establishment of H3K4me3 marks. Molecular and cellular biology 34, 464-473.

Langmead, B., Trapnell, C., Pop, M., and Salzberg, S.L. (2009). Ultrafast and memory-efficient alignment of short DNA sequences to the human genome. Genome biology 10, R25.

Matys, V., Kel-Margoulis, O.V., Fricke, E., Liebich, I., Land, S., Barre-Dirrie, A., Reuter, I., Chekmenev, D., Krull, M., Hornischer, K., et al. (2006). TRANSFAC and its module TRANSCompel: transcriptional gene regulation in eukaryotes. Nucleic acids research 34, D108-110.

Robinson, M.D., McCarthy, D.J., and Smyth, G.K. (2010). edgeR: a Bioconductor package for differential expression analysis of digital gene expression data. Bioinformatics 26, 139-140.

Sandelin, A., Alkema, W., Engstrom, P., Wasserman, W.W., and Lenhard, B. (2004). JASPAR: an open-access database for eukaryotic transcription factor binding profiles. Nucleic acids research 32, D91-94.

Smith, A.D., Chung, W.Y., Hodges, E., Kendall, J., Hannon, G., Hicks, J., Xuan, Z., and Zhang, M.Q. (2009). Updates to the RMAP short-read mapping software. Bioinformatics 25, 2841-2842.

Smith, A.D., Sumazin, P., Xuan, Z., and Zhang, M.Q. (2006). DNA motifs in human and mouse proximal promoters predict tissue-specific expression. Proceedings of the National Academy of Sciences of the United States of America 103, 6275-6280.

Supplemental legends

Figure S1, related to Figure 1. **Quantification of mammary ductal structures.** (A) H&E images of untreated and pellet-bearing mice. Mammary glands were harvested, paraffin-embedded, H&E stained. Stained slides were scanned on Aperio scanner (Leica Biosystems). (B) Mammary gland ductal quantifications. The number of ductal structures was determined from H&E images of untreated and pellet-bearing mice.

Figure S2, related to Figure 2. Mammary reference methylomes. (A) Representative example of methylation levels and HMR distribution across a basal-specific gene (Cytokeratin K5, Krt5) and luminal-specific gene (Cytokeratin K8, Krt8).

Figure S3, related to Figure 3. Parity induced methylation changes. (A) Representative example of parity-induced changes at the Dst gene locus, across nulliparous and parous mammary methylomes. (B) Pie chart depicting relative proportions of parous and nulliparous DMRs in promoter, genic, and intergenic regions. (C) Average DNA methylation levels of parous luminal DMRs in luminal cells 2 months after pregnancy, nulliparous luminal cells, and luminal cells post pseudo-pregnancy.(D) Cartoon illustrating some gene categories associated parous DMRs.

Figure S4, related to Figure 3. **Parity induced DMRs** (A) Representative examples of parity-induced changes at Itga6, Stat5a, Tgfbr2, Wnt5b loci, across nulliparous and parous luminal methylomes.

Figure S5, related to Figure 3. **Analysis of parous luminal DMRs and RRBS libraries.** Tukey boxplots demonstrate the average DNA methylation levels of parous luminal DMRs in luminal cells 2 months after pregnancy, nulliparous luminal cells, and RRBS libraries (day 10 pregnant mature, progenitor and stem, day 16 pregnant mature, progenitor and stem, day 19 pregnant mature, progenitor and stem, retired mature, progenitor and stem, virgin week 3 mature, progenitor and stem, virgin week 9 mature, progenitor and stem).

Figure S6, related to Figure 3. Methylation scores of Stat5a peaks that do not overlap with HMRs. Each score represents the difference between average methylation of the peak region in luminal parous and luminal nulliparous methylomes.

Figure S7, related to Figure 4. qPCR analysis of genes with unaltered DNA methylation status after pregnancy. qPCR analysis is shown for nulliparous and parous mice at day 6 and 12 after implantation of hormone pellets. All changes were significant to at least $p<0.05$.

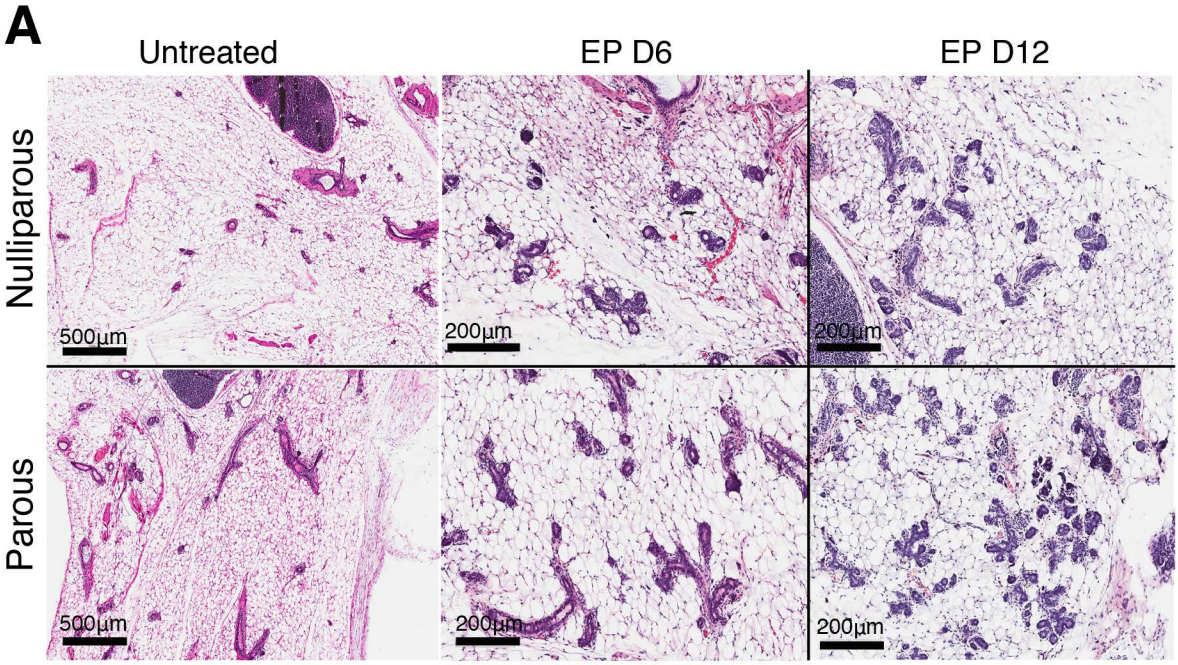

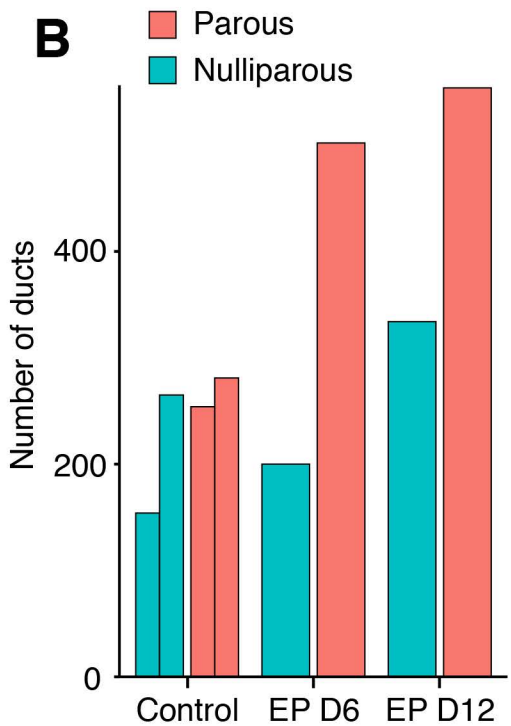

dos Santos & Dolzhenko et al., Figure S1

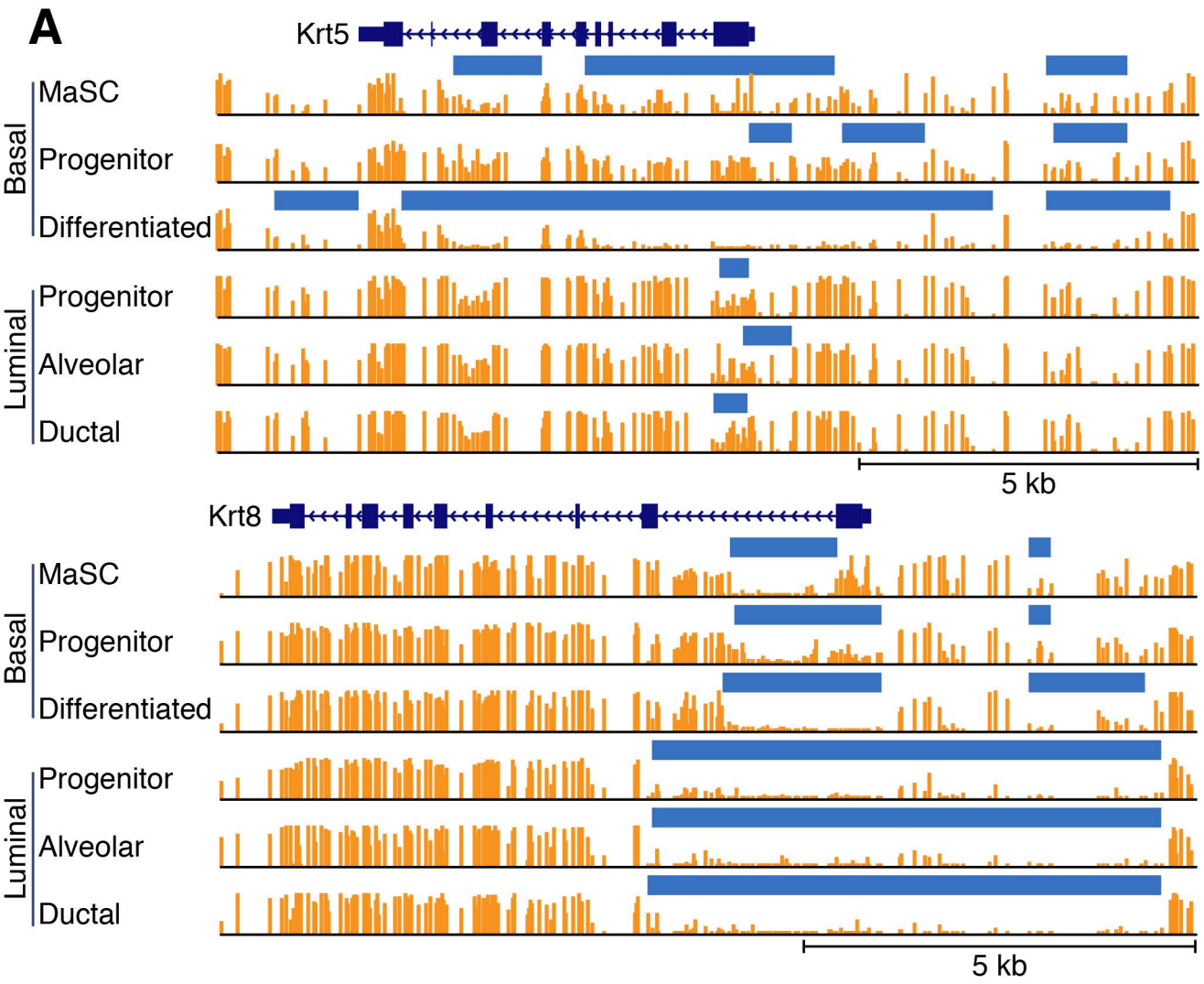

dos Santos & Dolzhenko et al., Figure S2

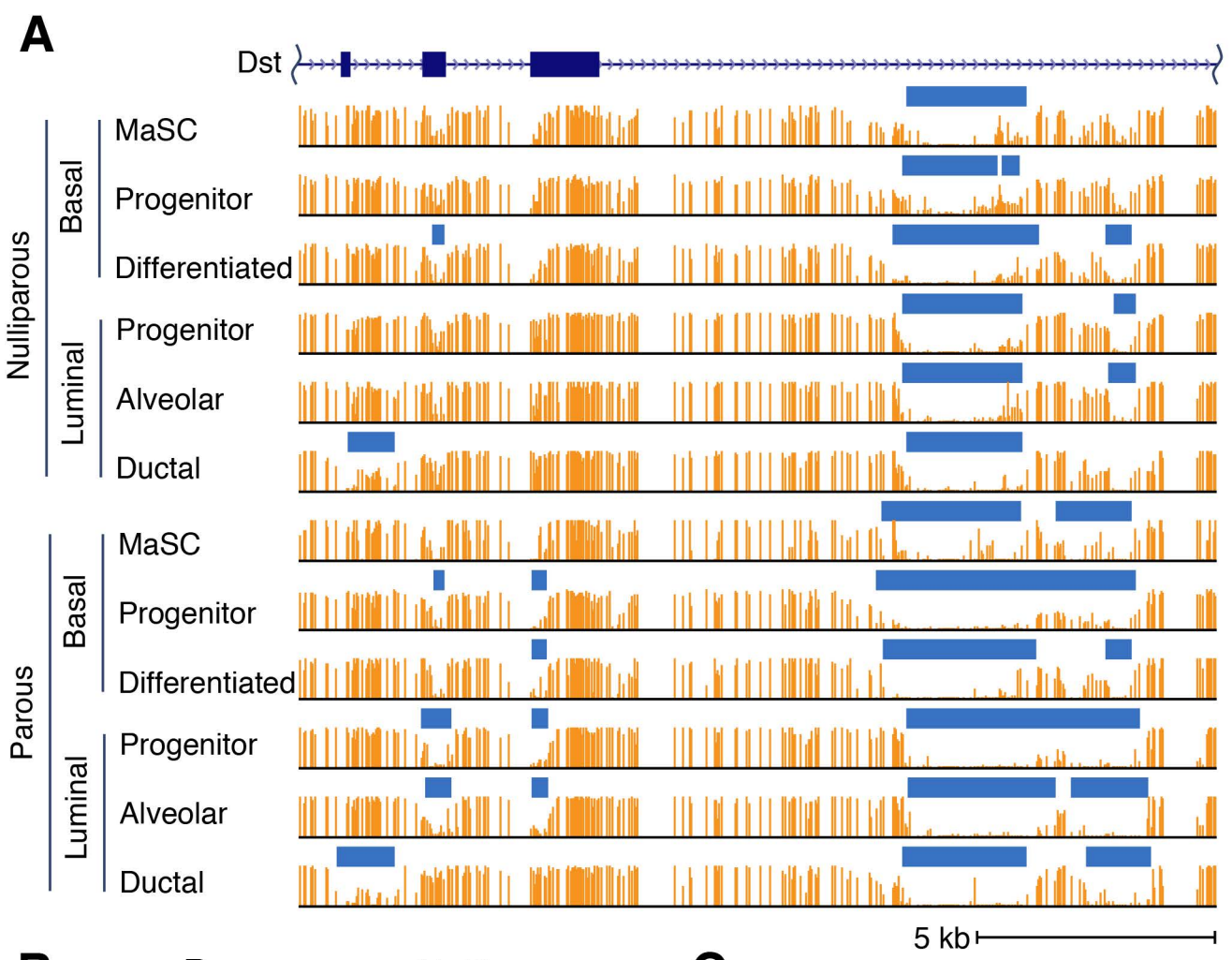

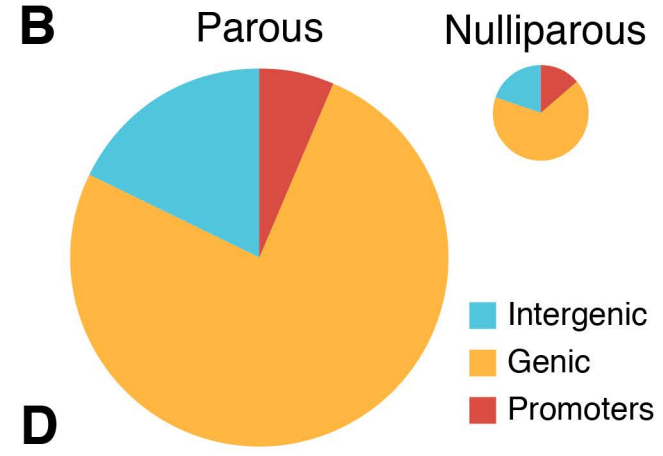

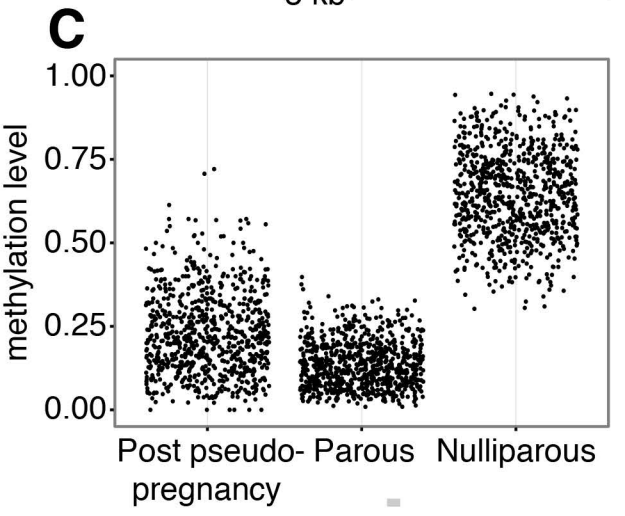

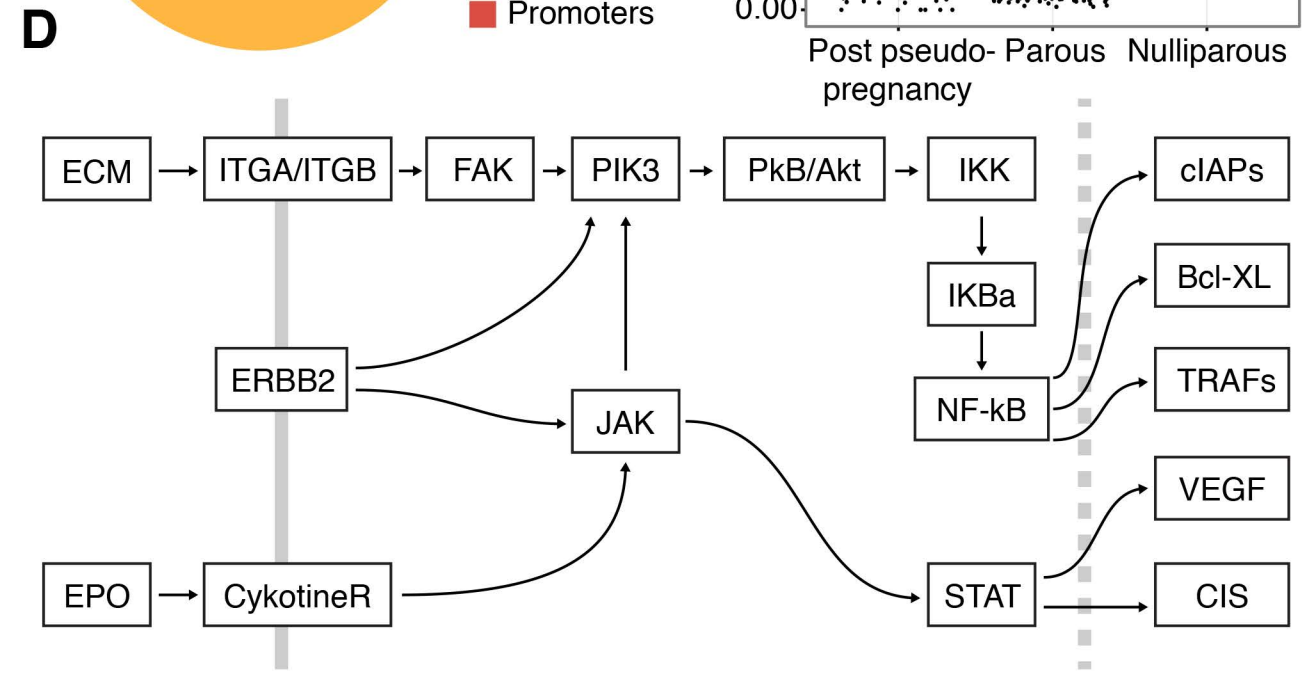

dos Santos & Dolzhenko et al., Figure S3

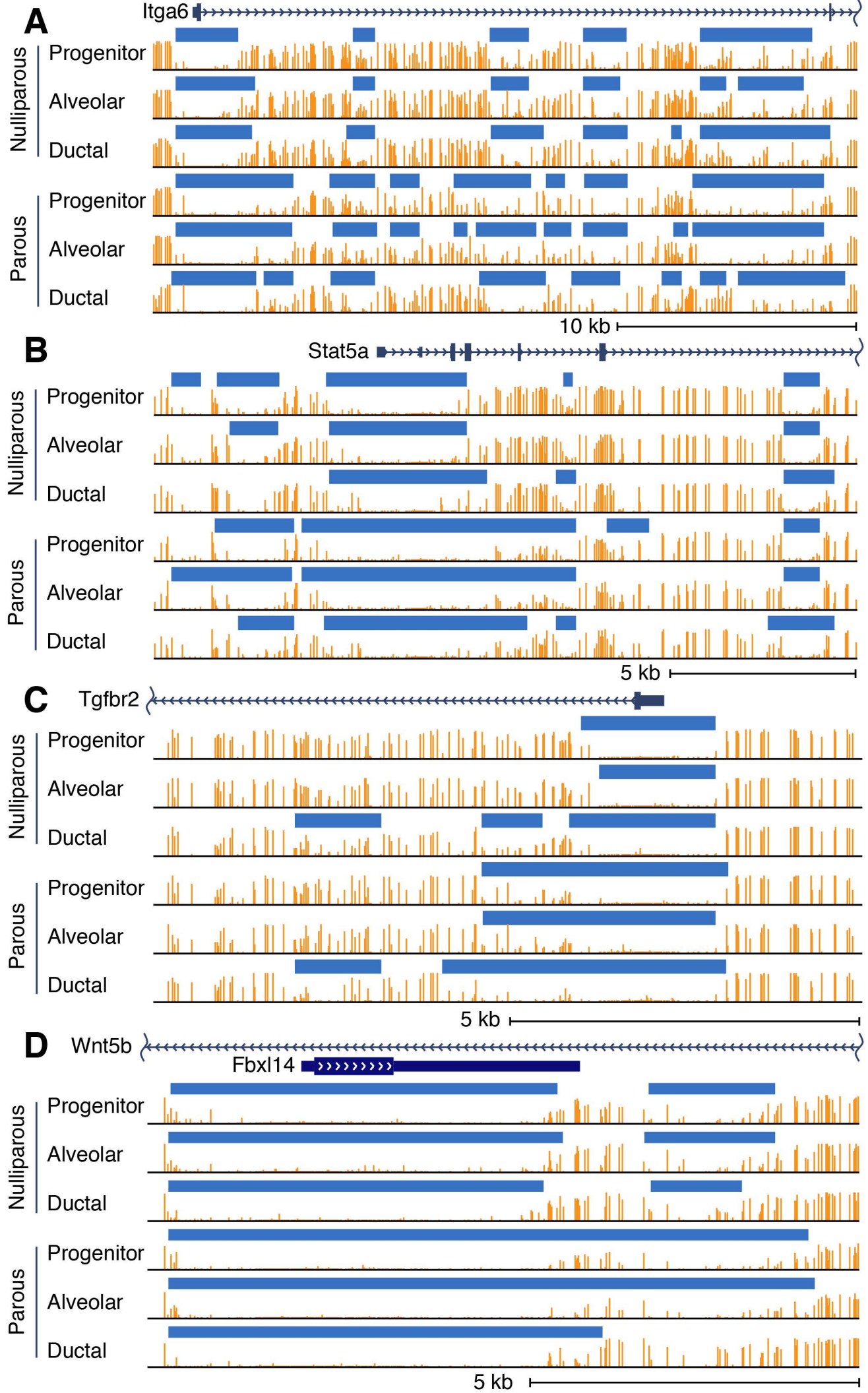

dos Santos & Dolzhenko et al., Figure S4

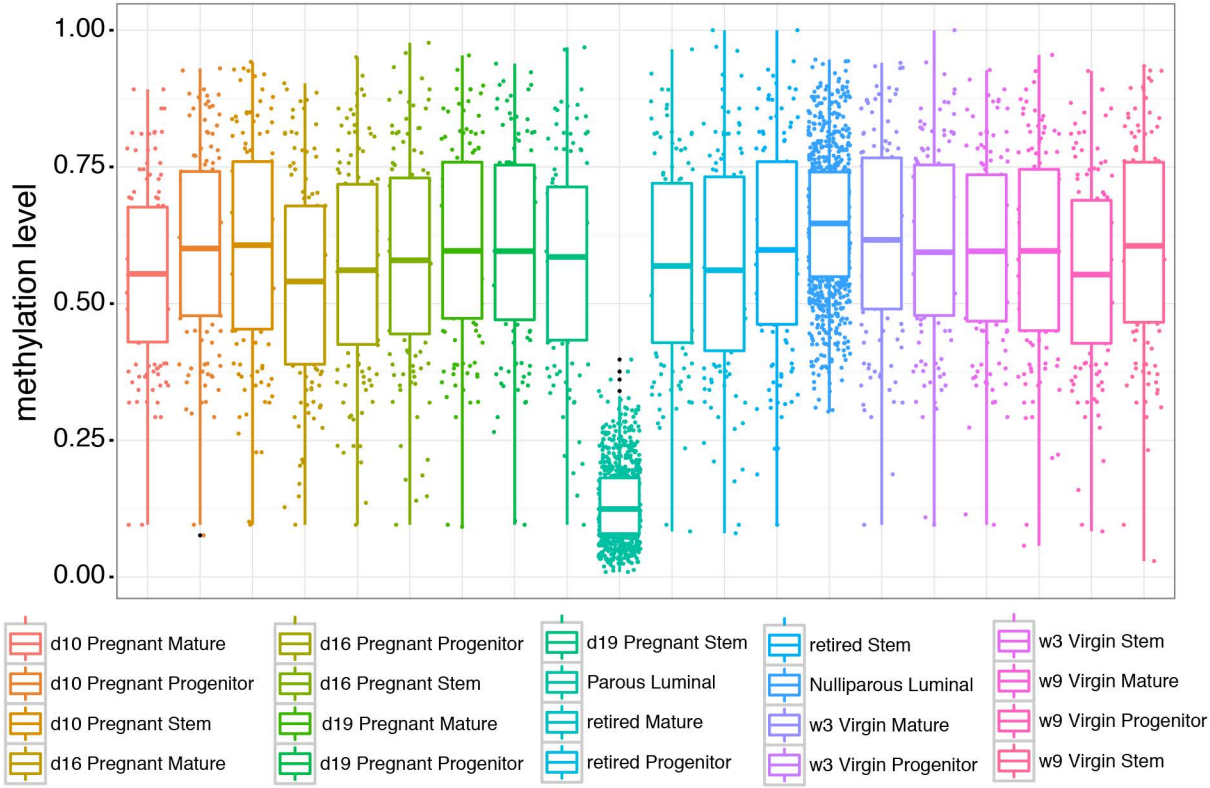

dos Santos & Dolzhenko et al., Figure S5

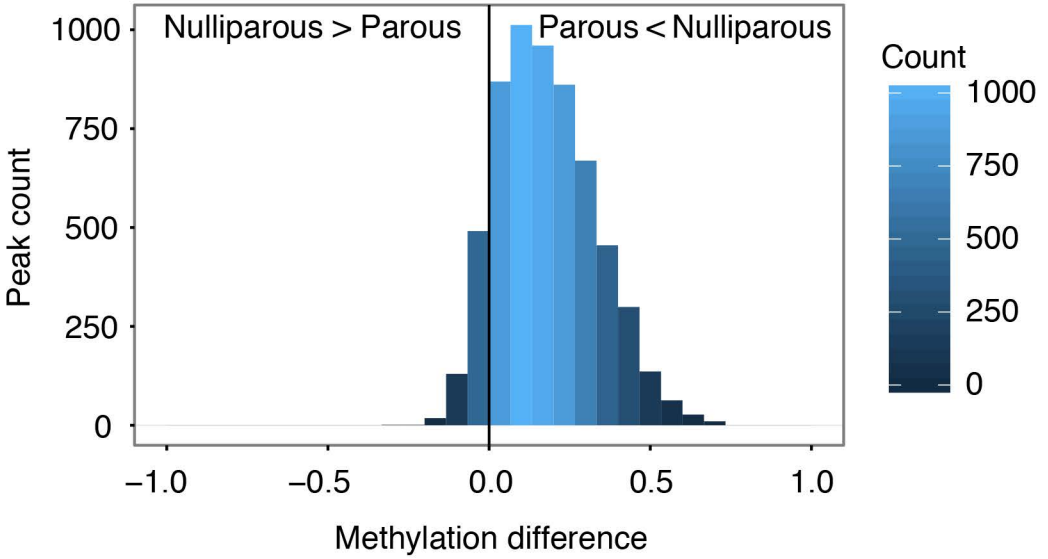

dos Santos & Dolzhenko et al., Figure S6

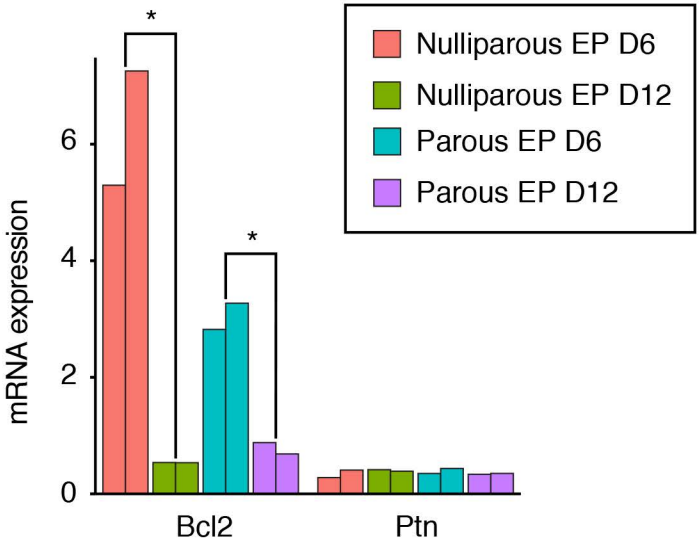

dos Santos & Dolzhenko et al., Figure S7